Hydrol. Earth Syst. Sci. Discuss., 9, 12395–12433, 2012
www.hydrol-earth-syst-sci-discuss.net/9/12395/2012/
doi:10.5194/hessd-9-12395-2012

Hydrology and
Earth System
Sciences
Discussions

Drought risk assessments of water resources systems under climate change: a case study in Southern Taiwan

T. C. Yang, C. Chen, C. M. Kuo, H. W. Tseng, and P. S. Yu

Department of Hydraulic and Ocean Engineering, National Cheng Kung University, No. 1, University Rd., Tainan 701, Taiwan

Received: 1 October 2012 – Accepted: 25 October 2012 – Published: 5 November 2012

Correspondence to: P. S. Yu (yups@mail.ncku.edu.tw)

Published by Copernicus Publications on behalf of the European Geosciences Union.

Title Page
Abstract | Introduction
Conclusions | References
Tables | Figures
◂◂ | ▸▸
◂ | ▸
Back | Close
Full Screen / Esc
Printer-friendly Version
Interactive Discussion

Abstract

This study aims at assessing the impact of climate change on drought risk in a water resources system in Southern Taiwan by integrating the weather generator, hydrological model and simulation model of reservoir operation. Three composite indices with multi-aspect measurements of reservoir performance (i.e. reliability, resilience and vulnerability) were compared by their monotonic behaviors to find a suitable one for the study area. The suitable performance index was then validated by the historical drought events and proven to have the capability of being a drought risk index in the study area. The downscaling results under A1B emission scenario from seven general circulation models were used in this work. The projected results show that the average monthly mean inflows during the dry season tend to decrease from the baseline period (1980–1999) to the future period (2020–2039); the average monthly mean inflows during the wet season may increase/decrease in the future. Based on the drought risk index, the analysis results for public and agricultural water uses show that the occurrence frequency of drought may increase and the severity of drought may be more serious during the future period than during the baseline period, which makes a big challenge on water supply and allocation for the authorities of reservoir in Southern Taiwan.

1 Introduction

According to the fourth assessment report of Intergovernmental Panel on Climate Change (IPCC, 2007), climate change causes that the atmospheric temperature and sea surface temperature increase. Besides, the occurrence frequency and severity of extreme weather (e.g. droughts and ~~furious~~ storms) have been considerably raised. The report (IPCC, 2007) also indicates that by the end of the century, climate change will place between 1.1 and 3.2 billion people at risk of water shortages. As we know, water shortages seriously affect the cities' social and economic development. Therefore, assessing impacts of climate change on water shortages for water management has become an important world-~~wild~~ issue recently (Vano et al., 2010; Hall and Murphy, 2010; Schilling et al., 2012; Hanak and Lund, 2012).

In Southern Taiwan, Yu et al. (2004, 2006) found that annual rainfall has decreased significantly during the past century. The studies (Tseng et al., 2012; Yu et al., 2004, 2010; Chen et al., 2009) pertaining to impacts of climate change on droughts point out that the occurrence frequency of meteorological and hydrologic droughts, the number of dry days, and the maximum consecutive dry days may increase obviously in the future, which ~~let~~ Southern Taiwan have to face ~~the~~ possible water shortage and ~~make~~ a big challenge to the ~~authorities~~ of reservoir ~~on~~ water supply and allocation. Tseng-wen Reservoir is located in Southern Taiwan and the largest water storage facility in Taiwan. The annual ~~total~~ water supply amount is 1047 million tons for different water ~~demands~~. Nearly 85 % of annual rainfall is concentrated in the wet season (from May to October), which makes the wet and dry seasons ~~obviously~~ distinct in the area. Hence, this reservoir plays an important role ~~to provide~~ functions on flood mitigation and water supply in the water resources system. Under climate change, however, the ~~following~~ change of hydrology processes in the catchment of reservoir ~~would~~ influence inflows ~~of~~ reservoir. The ~~following~~ changes of inflow would further influence reservoir storage, water supply and water shortage ~~in a water resources system~~. Therefore, assessing the changes of inflow, reservoir storage, water supply and water shortage in the future are essential to the authorities ~~of~~ reservoir for ~~making~~ suitable adaptation strategies to respond to the impacts of a changing climate.

Besides, in order to assess the impact of climate change on drought risk ~~in a water resources system~~, a suitable performance index is ~~necessary~~ which is able to quantify the characteristics of water shortage and be a drought risk index. The notion of drought has several meanings (Mishra and Singh, 2010). For example, meteorological drought (deficit in precipitation), agricultural drought (deficit in soil water), hydrological drought (deficit in river discharge), groundwater drought (deficit in groundwater storage), and socio-economic drought (conflict ~~of~~ water shortage and water management ~~demands~~). In our study, drought is the operational drought, that is, a period during which water shortage happens in a water resources system. Indexes represent aggregate measures of a combination of performance measures. Several indices have been developed specifically for water resources, such as the drought risk index (DRI) (Zongxue et al., 1998), the Palmer drought severity index (Palmer, 1965), water quality index (Brown et al., 1972), fairness (Lence et al., 1997), reversibility (Fanai and Burn, 1997), and consensus (Takeuchi et al., 1998). To quantify the sustainability of water resources systems, Loucks (1997) proposed the sustainability index (SUI), with the objective to facilitate the evaluation and comparison of water management policies. The SUI has been used by many researchers (Sandoval-Solis et al., 2011; Ray et al., 2010; McMahon et al., 2006; Loucks, 1997). The DRI and SUI summarize essential performance parameters of water management in a meaningful manner (i.e. reliability, resilience and vulnerability) and can be used to be drought risk indices to quantify the characteristics of water shortage in a water resources system. In our study, three indices (i.e. DRI, SUI and a modified SUI) were adopted. Performances of these three indices were compared by their monotonic behaviors to find a suitable one for the study area.

This study aims to find a suitable drought risk index which is capable of multi-aspect description of water shortage (including duration, number and severity) and assess the impact of climate change on reservoir inflow, reservoir storage, water supply and water shortage in the water resources system. The rest part of this paper is organized as follows: Sect. 2 "Study area and data set" provides a summary description of the study area and the data set. Section 3 "Methodologies" lists the models and indices which comprise weather generator, hydrological model, simulation model of reservoir operation and performance indices of water resources system (including single and composite indices). Section 4 "Analysis results" makes calibration and validation of hydrological model in the reservoir catchment in Sect. 4.1; comparisons of composite index in Sect. 4.2 to find the most suitable one; drought classification by the most suitable index and validation by historical events in Sect. 4.3 to test the index's ability; and impact assessment of climate change on reservoir inflow, reservoir storage, water supply and drought risk in Sect. 4.4. Finally, Sect. 5 "Conclusions" concludes the paper and gives some future work.

2 Study area and data set

Tsengwen Reservoir, completed in 1973 with a storage capacity of about 7.8×10^8 m^3, is the largest reservoir in Taiwan and has multifunction of water supplies for agricultural water use, industrial water use, public water use, flood control and hydropower generation. The annual total water supply amount is 1047 million tons. The catchment of Tsengwen Reservoir encloses an area of 481 km^2 and is at an elevation of from 157 to 3514 m above sea level. The locations of the study area, the reservoir and the raingauges are displayed in Fig. 1a. For this area, the mean annual precipitation is about 2740 mm, of which 85 % occurs during the wet season (from May to October) as shown in Fig. 1b.

Daily hydrological data, including rainfall, streamflow and temperature, continuously from 1975 to 2008 were used as the data set. The daily streamflow data are the inflow of Tsengwen Reservoir. The daily rainfall data were collected from the nine raingauges from which areal precipitations on the reservoir catchment were computed using the Thiessen polygon method. The daily mean temperature data were collected from two meteorological stations (i.e. Tsengwen and A-Li-Shan stations) from which the two stations' daily data in a day were averaged as the representative temperature of the reservoir catchment.

In the study, the future period is set to 2020–2039 and the baseline period is set to 1980–1999. Taiwan Climate Change Projection and Information Platform Project (TCCIP) (National Science Council of Taiwan, 2010) provides the downscaling projections of monthly rainfall and monthly mean temperature from the 24 general circulation models (GCMs) for each node of a 25 km × 25 km grid (covering Taiwan) under A1B, B1, and A2 emission scenarios. Besides, for each GCM, each grid node and each month, the change rates (%) of monthly rainfall and monthly mean temperature from the baseline period to the future period are also provided. Seven GCMs that are reported to properly consider the tropical cyclone information and East Asian Monsoon modeling, as mentioned in the study of Chu and Yu (2010), were used in this work. Table 1 gives the information about seven used GCMs in this study. The seven GCMs include CGCM3.1(T63), CSIRO-Mk3.5, ECHAM5/MPI-OM, GFDL-CM2.0, GFDL-CM2.1, MRI-CGCM2.3.2, and MIROC3.2(hires). In the study, only the A1B emission scenario was chosen. The change rates (%) of monthly rainfall and monthly mean temperature from the baseline period to the future period for these seven GCMs are listed in Table 2 and Table 3.

3 Methodologies

3.1 Weather generator

The daily precipitation generation is based on procedures proposed by Richardson (1981). The generator uses a Markov chain to model the occurrence of wet or dry days, and then uses a probability distribution to generate the precipitation amount conditional on a wet day modeled by the Markov chain. A first-order two-state Markov chain was used in this work. The occurrence of a dry or wet day is modeled by a transition probability matrix consisting of conditional probabilities, given a previous dry or wet day.

Many probability distributions were applied to generate daily precipitation amount, such as the exponential distribution (Selker et al., 1990; Tung et al., 1995), Weibull distribution (Yu et al., 2002), two-parameter gamma distribution (Richardson, 1981; Coe et al., 1982; Woolhiser et al., 1982; Schubert, 1994; Corte-Real et al., 1999), and mixed exponential distribution (Woolhiser et al., 1979, 1982, 1986). Among the probability distributions, the Weibull distribution most appropriately approximates daily rainfall in Taiwan (Yu et al., 2002); consequently, this work used the Weibull distribution to generate daily rainfall.

Regarding the daily temperature generation, a first-order autoregressive model was utilized to generate the daily temperature sequences in each month. This daily temperature generation model is expressed as follows:

$$T_k = \mu_T + \rho_{1T}(T_{k-1} - \mu_T) + \sqrt{1-\rho_{1T}^2}\sigma_T v_k + \Delta\mu \quad (1)$$

where T_k is the temperature on day k; μ_T is the mean temperature in a certain month; σ_T is the standard deviation of daily temperature in the month; ρ_{1T} is the lag-one autocorrelation coefficient of daily temperature in the month; v_k is the random standard normal variate, and $\Delta\mu$ is the mean temperature change in the month under a future scenario. Given the parameters, μ_T, σ_T, ρ_{1T}, and $\Delta\mu$, a daily temperature sequence in a month can be generated by this model.

3.2 Hydrological model

A continuous hydrologic model was used to simulate future projected streamflow, after the daily precipitation and temperature were obtained in the previous section by the downscaling method. This work used a continuous hydrologic model based on the structure of HBV hydrological model (Bergström, 1976, 1992), which was initially designed for use in Scandinavian catchments by the Swedish meteorological and hydrological institute. Yu and Yang (2000) adapted the HBV hydrological model structure to suit catchments in Taiwan. The HBV-based hydrological model uses both an upper and lower tanks to model the rainfall-runoff behavior. Model structure mainly consists of three parts: (1) soil moisture module, (2) runoff response mechanism, and (3) water balance functions. Detail description of the HBV-based hydrological model, as well as its procedures for calibration and validation in this work, can be found in Yu and Yang (2000) and Yu et al. (2002).

In the HBV-based hydrological model, Hamon's temperature-dependent equation (Hamon, 1961) was used to transform the daily temperature series into the daily potential evapotranspirartion series. The Hamon's temperature-dependent equation is as:

$$\mathrm{Ep}_t = 0.021 H_t^2 e_t / [T_t + 273] \tag{2}$$

where Ep_t is the potential evapotranspiration (cm day^{-1}) on day t; H_t is the sunshine duration (h) on day t; e_t is the saturated vapor pressure (milibar) on day t; T_t is the mean temperature (°C) on day t. The value of e_t can be estimated by the following empirical equation:

$$e_t = 33.8639 \times [(0.00738T_t + 0.8072)^8 - 0.000019 \times |1.8T_t + 48| + 0.001316] \tag{3}$$

3.3 Simulation model of reservoir operation

The daily inflow time series are routed through a reservoir system for simulating water supply process. The reservoir system can be described by the following continuity equation. The equation considers the inflow, draft, evaporation and storage of reservoir in each time period.

$$S_{t+1} = S_t + I_t - O_t - E_t \tag{4}$$

$$S_{t+1} = \begin{cases} S_{\max} \; ; Q_t^{\mathrm{over}} = S_{t+1} - S_{\max} & ;\text{if} \quad S_{t+1} > S_{\max} \\ S_{t+1} \; ; Q_t^{\mathrm{over}} = 0 & ;\text{if} \quad S_{t+1} \le S_{\max} \end{cases} \tag{5}$$

where S_{t+1} is the storage of reservoir in time period $t+1$; S_t is the storage of reservoir in time period t ; I_t and E_t represent inflow and evaporation loss for the reservoir in time period t ; S_t is the storage of reservoir which can vary from 0 to $S_{\max}$ (i.e. storage capacity); O_t is the draft from the reservoir for different water uses (i.e. $O_t = \mathrm{DO}_t + \mathrm{IAO}_t$); Q_t^{over} is the spill; $S_{\max}$ is the storage capacity of reservoir; DO_t is the draft for domestic water use; IAO_t is the draft for industrial and agricultural water uses.

The drafts from Tsengwen Reservoir are decided by the reservoir storage and the operation rule curves (Fig. 2). The drafts for domestic water use (DO_t) and industrial and agricultural water uses (IAO_t) are based on the following rules:

$$\mathrm{DO}_t = \mathrm{DD}_t,\ \mathrm{IAO}_t = \mathrm{IAD}_t;\ \text{if } S_t > L_{\text{upper}} \quad (6)$$

$$\mathrm{DO}_t = \mathrm{DD}_t,\ \mathrm{IAO}_t = \mathrm{IAD}_t;\ \text{if } L_{\text{upper}} > S_t > L_{\text{middle}} \quad (7)$$

$$\mathrm{DO}_t = A_1 \times \mathrm{DD}_t,\ \mathrm{IAO}_t = A_2 \times \mathrm{IAD}_t;\ \text{if } L_{\text{middle}} > S_t > L_{\text{lower}} \quad (8)$$

$$\mathrm{DO}_t = B_1 \times \mathrm{DD}_t,\ \mathrm{IAO}_t = B_2 \times \mathrm{IAD}_t;\ \text{if } L_{\text{lower}} > S_t > S_{\text{min}} \quad (9)$$

$$\mathrm{DO}_t = \mathrm{IAD}_t = 0,\ \text{if } S_{\text{min}} > S_t \quad (10)$$

where DO_t is the draft for domestic water use; DD_t is the demand for domestic water use; IAO_t is the draft for industrial and agricultural water uses; IAD_t is the demand for industrial and agricultural water uses; S_t is the reservoir storage; L_{upper} is the upper limit of rule curve; L_{middle} is the middle limit of rule curve; L_{lower} is the lower limit of rule curve; S_{min} is the dead storage of reservoir; A_1 is the rate of discount for public water use when $L_{\text{middle}} > S_t > L_{\text{lower}}$; A_2 is the rate of discount for agricultural and industrial water uses when $L_{\text{middle}} > S_t > L_{\text{lower}}$; B_1 is the rate of discount for public water use when $L_{\text{lower}} > S_t$; B_2 is the rate of discount for agricultural and industrial water uses when $L_{\text{lower}} > S_t$.

Figure 3 shows demands of agricultural, industrial, and domestic water uses. These demands will be fully supplied when the water of reservoir is abundant. Otherwise, the supplies will be reduced when the water of reservoir is scarce.

3.4 Performance indices of water resources system

3.4.1 Single indices

Generally, failures in the operation of a reservoir have many aspects: extent, number, severity (Jain, 2010). In the following, the single indices (i.e. reliability, resilience and vulnerability) which are used to measure different aspects of the performance of a reservoir are described. Usually these single indices are computed using daily, monthly or annual data for the operation of the system. In the study, the daily data were used. The following description of the single indices is based on the assumption that the system under consideration at a given time t can be in either a satisfactory (i.e. non-failure, NF) state or an unsatisfactory (i.e. failure, F) state. In this study the focus is on water resources systems. Therefore, the NF state occurs when water supply is able to meet water demand and, hence, the F state is when supply cannot meet demand.

Reliability

Water supply reliability is the probability that the available water supply meets the water demand during the period of simulation (Klemes et al., 1981; Hashimoto et al., 1982). For each time period t, deficit D_t is positive when the water demand X_{D_t} is more than the water supply X_{S_t}; if the water supply is equal to water demand ($X_{D_t} = X_{S_t}$), deficit is zero ($D_t = 0$) (Loucks, 1997).

$$D_t = \begin{cases} X_{D_t} - X_{S_t} & \text{if } X_{D_t} > X_{S_t} \\ 0 & \text{if } X_{D_t} = X_{S_t} \end{cases} \tag{11}$$

The most widely accepted and applied definition for water resources systems is occurrence reliability (Hashimoto et al., 1982), which is the portion of time that the water demand is fully supplied (i.e. non-failure state, NF) and can be estimated as:

$$\text{Rel} = 1 - \frac{\text{No. of days } D_t > 0}{n} \tag{12}$$

where D_t is water deficit on day t and n is the total number of time intervals (days).

Resilience

Resilience (Res) is a measure of how fast a system is likely to return to a satisfactory state (i.e. NF state) once the system has entered an unsatisfactory state (i.e. F state). Hashimoto et al. (1982) define resilience as a conditional probability:

$$\text{Res} = \frac{P\left\{S_t \in \text{NF}, S_{t-1} \in \text{F}\right\}}{P\left\{S_t \in \text{F}\right\}} \tag{13}$$

where S_t is the system state variable under consideration. Moy et al. (1986) used the maximum number of consecutive deficit periods prior to recovery as an alternative definition of resilience. Resilience is the probability that a successful period follows a failure period (the number of times $D_t = 0$ follows $D_t > 0$) for all failure periods (the number of times $D_t > 0$ occurred). This statistic assesses the recovery of the system once it has failed:

$$\text{Res} = \frac{\text{No. of days } D_t = 0 \text{ follows } D_t > 0}{\text{No. of days } D_t > 0 \text{ occurred}} \tag{14}$$

where D_t is water deficit on day t.

Vulnerability

Vulnerability expresses the severity of failures. Vulnerability can be expressed as (1) the average failure (Loucks and van Beek, 2005; Sandoval-Solis et al., 2011); (2) the average of maximum shortfalls over all continuous failure periods (Hashimoto et al., 1982; McMahon et al., 2006); and (3) the probability of exceeding a certain deficit threshold (Mendoza et al., 1997). This paper uses the first approach, the expected value of deficits, which is the sum of the deficits, D_t, divided by the deficit period, the number of times (days) $D_t > 0$ occurred. Dimensionless vulnerability is calculated by dividing the average daily deficit by the average daily water demand (WD):

$$\text{Vul} = \frac{\left(\sum_{t=0}^{t=n} D_t\right) / \text{No. of days } D_t > 0 \text{ occurred}}{\text{WD}} \tag{15}$$

where D_t is water deficit on day t and n is the total number of time intervals (days); WD is the average daily water demand.

3.4.2 Composite indices

The single indices (i.e. reliability, resilience and vulnerability) which are used to measure different aspects of the performance of a reservoir. Reliability, resilience and vulnerability imply the extent, number, and severity of water shortage events. In the recent past, some attempts (Loucks, 1997; Zongxue et al., 1998) have been made to quantitatively represent sustainability of water resources managements by using the composite indices which are composed of the three single indices. Composite indices are more efficient than single indices which can measure various characteristics of drought event.

Zongxue et al. (1998) proposed an integrated risk index, drought risk index (DRI), as a linear weighted function of reliability and resiliency and vulnerability.

$$\mathrm{DRI} = \frac{1}{3}(1-\mathrm{Rel}) + \frac{1}{3}(1-\mathrm{Res}) + \frac{1}{3}\mathrm{Vul} \tag{16}$$

where Rel is reliability; Res is resilience; Vul is vulnerability. The DRI's values vary from 0–1 and the value closer to 1 means the condition of water shortage is more serious.

Loucks (1997) proposed the sustainability index (SUI), which has the following properties: (1) its values vary from 0–1; (2) if one of the performance criteria is zero, the sustainability will be zero also; and (3) there is an implicit weighting because the index gives added weight to the criteria with the worst performance. The multiplicative form of the index considers each criterion as essential and nonsubstitutable. The SUI summarizes essential performance parameters of water management in a meaningful manner and the SUI has been used by the scientific community (Sandoval-Solis et al., 2011; Ray et al., 2010; McMahon et al., 2006; Loucks, 1997)

$$\mathrm{SUI} = [\mathrm{Rel} \times \mathrm{Res} \times (1-\mathrm{Vul})]^{\frac{1}{3}} \tag{17}$$

where Rel is reliability; Res is resilience; Vul is vulnerability. SUI's values vary from 0–1 and the value closer to 1 means the condition of water shortage is less serious. The study slightly modified the SUI into the following form (called MSUI) whose values vary from 0–1. As DRI, the MSUI's value closer to 1 means the condition of water shortage is more serious.

$$\text{MSUI} = [(1 - \text{Rel}) \times (1 - \text{Res}) \times \text{Vul}]^{\frac{1}{3}} \tag{18}$$

where Rel is reliability; Res is resilience; Vul is vulnerability. The study uses the three composite indices, including DRI, SUI and MSUI, for behavior analysis to choose a suitable one as the drought risk index for the study area.

4 Analysis results

4.1 Calibration and validation of HBV-based hydrological model

The HBV-based hydrological model was applied in the catchment of Tsengwen Reservoir for inflow simulation. The fuzzy multiple objective functions, proposed by Yu and Yang (2000), and the shuffled complex evolution optimization method (Duan et al., 1994) were adopted in the study. Historical daily rainfall, temperature, and inflow data from 1975 to 2000 were used for model calibration. The calibrated HBV-based hydrological model was further verified by historical data from 2001 to 2008. To assess the model performance, three criteria, including the ratio of the summation of simulated inflows to the summation of observed inflows (Ratio), the root mean squared error (RMSE), and the coefficient of correlation (CC) between simulated and observed daily inflows, were calculated for the calibration and verification periods, respectively. During the calibration period, the values of Ratio, RMSE and CC are 0.957, 6.849 (mm) and 0.938, respectively. During the validation period, the values of Ratio, RMSE and CC are 0.985, 9.539 (mm) and 0.964, respectively. Figure 4a, b show the calibration and verification results in 1976 and 2002, respectively. These results reveal the HBV-based hydrological model is able to simulate the rainfall-runoff behavior over the study area.

4.2 Comparisons of composite index

According to the researches (Jain, 2010; Kjeldsen and Rosbjerg, 2004), the water resource indices should have monotonic behaviors. The study investigated the degree of monotonic behavior of the three composite indices (DRI, SUI, and MSUI) for choosing a suitable one for the water resource system in the study area. The observed inflows have been used for analysis of monotonic behavior by estimating the three composite indices with changes in (1) evaporation, (2) water demand, (3) reservoir storage capacity and (4) reservoir inflow.

The analysis results of monotonic behavior for each index are shown in Fig. 5. The estimates of DRI exhibit monotonic behaviors in Fig. 5a as the water demand, reservoir storage capacity and reservoir inflow increase. However, the estimates of DRI exhibit a non-monotonic decrease as the evaporation increases in Fig. 5a. In Fig. 5b, the estimates of SUI generally exhibit non-monotonic behaviors as the estimates do not increase or decrease monotonously as the evaporation, water demand, reservoir storage capacity and reservoir inflow increase. In Fig. 5c, the estimates of MSUI exhibit monotonic behaviors as the estimates increase or decrease monotonously as the evaporation, water demand, reservoir storage capacity and reservoir inflow increase. Based on the above comparisons of monotonic behavior, MSUI performed the best and was chosen as the suitable index for the following analysis in the study area.

4.3 Drought classification by MSUI and validation by historical events

In order to classify the level of drought by MSUI, determining different thresholds of MSUI for different degrees of drought is necessary. The study refers to the drought classification standard, proposed by Water Resource Agency (WRA), Taiwan, for determining the thresholds of MSUI for different levels of drought. The drought classification standard of WRA is based on the deficit rates for public and agricultural water supplies. Here, the public water supply is defined as the sum of domestic and industrial water supplies. According to the standard of WRA, three intervals of deficit rate for public water supply, > 30 %, 20–30 % and 10–20 %, are defined as Level 1, Level 2 and Level 3, respectively; three intervals of deficit rate for agricultural water supply, > 50 %, 40–50 % and 30–40 %, are defined as Level 1, Level 2, Level 3. Moreover, the operation of Tsengwen Reservoir is based on a 10-day period. The water supplies from the reservoir are decided every 10-day period on the basis of operation rule curves. Hence, this work uses the time scale, 10-day period, for following calculation.

The value of MSUI, public and agricultural deficit rates for each 10-day period were computed from 1981 to 1999. For each drought level, the values of MSUI are displayed by using the box plot in Fig. 6a, b for public and agricultural water supplies, respectively. For each drought level, the median of MSUI value was used to determine the intervals of MSUI value for different drought levels as follows. For the public water supply system, the MSUI value of 0.8–1.0 is classified into Level 1; the MSUI value of 0.5–0.8 is classified into Level 2; and the MSUI value of 0.4–0.5 is classified into Level 3. For the agricultural water supply system, three intervals of MSUI value (i.e. 0.9–1.0, 0.8–0.9 and 0.7–0.8) were classified into Level 1, Level 2 and Level 3, respectively. Drought levels and their corresponding MSUI values and deficit rates are shown in Fig. 7.

In order to validate whether MSUI can judge drought event or not, the study used two periods (1981–1999 and 2000–2007) of historical drought events for validating and testing the MSUI's performances, respectively. During the historical drought periods, the percentage, p_x, of the 10-day number with MSUI $\geq x$ to the 10-day number of historical drought was calculated as

$$p_x = \frac{N_{(\mathrm{MSUI}\geq x|\mathrm{HD})}}{N_{\mathrm{HD}}} \tag{19}$$

where x is a threshold of MSUI, HD means historical drought period, N_{HD} indicates the 10-day number of historical drought, and $N_{(\mathrm{MSUI}\geq x|\mathrm{HD})}$ denotes the 10-day number with MSUI $\geq x$ during the historical drought periods.

The results during the validating period (1981–1999) are shown in Fig. 8. From the figure, when the threshold of MSUI (x) is less than or equal to 0.4, the percentage

(p_x) is the highest (i.e. $p_{0.1} = p_{0.2} = p_{0.3} = p_{0.4} = 79.12\,\%$). While, when the threshold of MSUI (x) is greater than 0.4, the percentage (p_x) decreases, which means that 0.4 is a threshold value of MSUI for catching most of the historical drought events. Moreover, the value of 0.4 is the same as the threshold of Drought Level 3 for public water supply system, which implies that the value of 0.4 is a reasonable threshold for the lowest level of drought. Further, the percentage for MSUI ≥ 0.4 (i.e. $p_{0.4}$) during the testing period (2000–2007) is 93.0 %, which also reveals that MSUI is effective as the indicator of drought risk assessment and used to determine the severity of water shortage and occurrence of drought event.

4.4 Impact assessment of climate change

4.4.1 Impact on rainfall, temperature and reservoir inflow

Using the change rates of monthly rainfall and monthly mean temperature in Table 2 and Table 3, the parameters in the weather generator (i.e. mean of Weibull distribution and μ_T in Eq. (1) have been adjusted for future rainfall and temperature generation. For each generation, 200 yr of daily rainfall/temperature are synthesized as projected scenario data. Then, these projected scenario data will be further compared with baseline data. The baseline data are also generated by weather generator but without consideration of climate change (the parameters in the weather generator are not be adjusted). The projected mean monthly rainfalls by different GCMs under A1B emission scenario are shown in Fig. 9a. The projected rainfall amounts by different GCMs vary from 318 mm to 388 mm during the dry season and from 1840 mm to 2408 mm during the wet season. The baseline rainfall amounts during the dry and wet seasons are 381 mm and 2167 mm, respectively. The results show that the rainfall amount during the dry season tends to decrease from the baseline period to the future period; while, the rainfall amount during the wet season has an uncertain trend which may increase or decrease from the baseline period to the future period. The projected average monthly mean temperatures by different GCMs under A1B emission scenario are shown in

Fig. 9b, which reveals the increases of projected average monthly mean temperatures by different GCMs in spring and winter are larger than in summer and autumn.

By using the above projected rainfalls and temperatures as input, the HBV-based hydrological model was performed to generate the reservoir inflows. Figure 9c shows the average monthly mean inflows during the baseline period and the future period. During the baseline period, the average monthly mean inflows during the dry and wet seasons are 6.01 $m^3 s^{-1}$ and 53.7 $m^3 s^{-1}$, respectively. The projected average monthly mean inflows by different GCMs vary from 3.34 $m^3 s^{-1}$ to 5.47 $m^3 s^{-1}$ during the dry season and from 43.8 $m^3 s^{-1}$ to 59.5 $m^3 s^{-1}$ during the wet season. The results show that the average monthly mean inflows during the dry season tend to decrease from the baseline period to the future period; while, the average monthly mean inflows during the wet season have an uncertain trend which may increase or decrease from the baseline period to the future period.

4.4.2 Impact on reservoir storage and water supply

Through the weather generator and the HBV-based hydrological model, the simulated inflows of reservoir have system errors resulted from uncertainties of model structure and parameters. In order to reduce system errors and keep the generated inflow temporal pattern close to the observed inflow temporal pattern, the study used the observed daily inflows during the baseline period (1980–1999) and the adjusted daily inflows during the future period (2020–2039) for simulation of reservoir system to investigate impacts of climate change on reservoir storage, water supply and drought risk The adjusted daily inflows during the future period were obtained by the adjusting factor as

$$C_{S_i} = \frac{Q_{S_i}}{Q_{B_i}} \tag{20}$$

where C_{S_i} is the adjusting factor for the ith month; Q_{S_i} is the generated mean monthly inflow in the ith month during the future period; Q_{B_i} is the generated mean monthly inflow in the ith month during the baseline period by using the weather generator and the HBV-based hydrological model. The adjusted daily inflows during the future period were obtained by using the observed daily inflows multiplied by the adjusting factor.

$$Q_{A_{i,j}} = Q_{O_{i,j}} \times C_{S_i} \tag{21}$$

where $Q_{A_{i,j}}$ is the adjusted daily inflows on the jth day in the ith month during the future period; $Q_{O_{i,j}}$ is the observed daily inflows on the jth day in the ith month during the baseline period; C_{S_i} is the adjusting factor for the ith month.

Through the simulation of reservoir operation, the mean monthly storages and water supply amounts during the baseline period and during the future period, respectively, were calculated. The percentage changes of mean monthly storage and mean monthly water supply amount from the baseline period to the future period are shown in Fig. 10 and Fig. 11, respectively. The figures reveal the decreases of storage and water supply amount are larger in April to June than in the other months. In May, the percentage change of storage ranges from −1.2 % to −37.8 % and the percentage change of water supply amount ranges from −0.3 % to −13.3 %.

4.4.3 Impact on drought risk

The values of MSUI for each 10-day period during the baseline and future periods were computed for public and agricultural water supply-demand systems, respectively. These values of MSUI for each 10-day period were then classified into different drought levels by using the intervals for different drought levels in Fig. 7. Figure 12a shows the numbers of 10-day period of different drought levels for public water supply-demand system during the baseline and future periods. In the figure, the numbers of 10-day period are 19 for Drought Level 1, 134 for Drought Level 2, and 16 for Drought Level 3 during the baseline period. By comparing the numbers of 10-day period for different drought levels during the baseline period and the future period under A1B emission scenario, the following results can be found: (1) the number of 10-day period for

Drought Level 2 increases a lot and is around 2.34 times of the number of 10-day period during the baseline period; (2) the total number of 10-day period (for Drought Levels 1, 2, and 3) is around 2.2 times of the total number of 10-day period during the baseline period. The aforementioned finding reveals that the number of 10-day period which satisfies the public water demand seems to decrease under the A1B emission scenario, which implies that the drought risk for public water use will rise in the future.

Figure 12b shows the numbers of 10-day period of different drought levels for agricultural water supply-demand system during the baseline and future periods. In the figure, the numbers of 10-day period are 14 for Drought Level 1, 5 for Drought Level 2, and 85 for Drought Level 3 during the baseline period. By comparing the numbers of 10-day period for different drought levels during the baseline period and the future period under A1B emission scenario, the following results can be found: (1) the number of 10-day period for Drought Level 3 increases a lot and is around 1.81 times of the numbers of 10-day period during the baseline period; (2) the total number of 10-day period (for Drought Levels 1, 2, and 3) is around 1.8 times of the total number of 10-day period during the baseline period. The aforementioned finding reveals that the number of 10-day period which satisfies the agricultural water demand seems to decrease under the A1B emission scenario, which implies that the drought risk for agricultural water use will rise in the future.

The above drought risk assessment reveals that the occurrence frequency of drought may increase and the severity of drought may be more serious during the future period than during the baseline period, which makes a big challenge on water supply and allocation for the authorities of reservoir in Southern Taiwan.

5 Conclusions

This study assessed the impact of climate change on the drought risk in a water resources system in Southern Taiwan. By integrating the weather generator, hydrological model, and reservoir system model, the reservoir inflows and drafts under the climate change scenario were generated. Through the performance index of water resources system, the impact of climate change on the drought risk was assessed.

Apart from previous studies using the shortage rate as the level of water shortage hazard, this study used three composite indices with multi-aspect description of water shortage, including duration, number and severity of water shortage. Composite indices are more efficient than single indices which can measure various characteristic of drought event. This kind of composite index can provide more information about drought events. Three composite performance indices (DRI, SUI, and MSUI) were compared by their monotonic behaviors to find a suitable one for the study area to assess the impact of climate change on the risk of water shortage. Each composite index is composed of three single indices (i.e. reliability, resilience and vulnerability) which are used to measure different aspects (i.e. the extent number, and severity) of water shortage events The MSUI was found to have monotonic behaviors with changes in (1) evaporation, (2) water demand, (3) reservoir storage capacity and (4) reservoir inflow, and be the most suitable one for the study area. The MSUI was then validated by the historical drought events and proven to have the capability of being the criterion of drought in the study area. Moreover, enhencing the link between composite indices and practical applications is very essential. In Taiwan, the present drought classification standard, proposed by WRA (Taiwan), considers only a varible (i.e. the deficit rate) for drought classification. Using composite indices (e.g. MSUI) as drought classification variables, which can measure different aspects of water shortage events, will be an important issue and the future work.

The downscaling results under A1B emission scenario from seven GCMs that consider the tropical cyclone information and East Asian Monsoon modeling were used in this work. The inflow projected results show that the average discharges during the dry season tends to decrease from the baseline period (1980–1999) to the future period (2020–2039); the average discharge during the wet season may increase/decrease from the baseline period to the future period.

From the analysis results of drought risk for public and agricultural water uses under A1B emission scenario, the total numbers of 10-day period for all drought levels are around 2.2 and 1.8 times of the total numbers of 10-day period during the baseline period, respectively. The results indicate the occurrence frequency of drought may increase and the severity of drought may be more serious during the future period than during the baseline period, which makes a big challenge on water supply and allocation for the authorities of reservoir in Southern Taiwan.

Acknowledgements. The authors would like to thank the National Science Council of the Republic of China (Taiwan) for financially supporting this research under Contract No. NSC 97-2221-E-006-150-MY3 and Taiwan Climate Change Projection and Information Platform Project (TCCIP) for offering future precipitation projections.

References

Bergström, S.: Development and application of a conceptual runoff model for Scandinavian Catchments, SMHI, Reports RHO. 7, Norrköping, 1976.

Bergström, S.: The HBV model – its structure and applications, SMHI, Reports RHO. 4, Norrköping, 1992.

Brown, R. M., McClelland, N. I., Deininger, R. A., and O'Connor, M. F.: A Water Quality Index – Crashing the Psychological Barrier, Indicators of Environmental Quality, Plenum, New York, 1972.

Chen, S. T., Kuo, C. C., and Yu, P. S.: Historical trends and variability of meteorological droughts in Taiwan, Hydrolog. Sci. J., 54, 430–441, 2009.

Chu, J. L. and Yu, P. S.: A study of the impact of climate change on local precipitation using statistical downscaling, J. Geophys. Res., 115, D10105, doi:10.1029/2009JD012357, 2010.

Coe, R. and Stern, R. D.: Fitting models to rainfall data, J. Appl. Meteorol., 21, 1024–1031, 1982.

Corte-Real, J., Xu, H., and Qian, B.: A weather generator for obtaining daily precipitation scenarios based on circulation patterns, Climate Res., 13, 61–75, 1999.

Duan, Q., Sorooshian, S., and Gupta, V. K.: Optimal use of the SCE-UA global optimisation method for calibrating watershed models, J. Hydrol., 158, 265–284, 1994.

Fanai, N. and Burn, D. H.: Reversibility as a sustainability criterion for project selection, Int. J. Sust. Dev. World, 4, 259–273, 1997.

Hall, J. and Murphy, C.: Vulnerability analysis of future public water supply under changing climate conditions: a study of the Moy catchment, Western Ireland, Water Resour. Manag., 24, 3527–3545, 2010.

Hamon, W. R.: Estimating potential evapotranspiration, J. Hydr. Eng. Div.-ASCE, 871, 107–120, 1961.

Hanak, E. and Lund, J. R.: Adapting California's water mangement to climate change, Climatic Change, 111, 17–44, 2012.

Hashimoto, T., Stedinger, J. R., and Loucks, D. P.: Reliability, resiliency, and vulnerability criteria for water-resource system performance evaluation, Water Resour. Res., 18, 14–20, 1982.

IPCC: Climate Change 2007: The Physical Science Basis, The Fourth Assessment Report, 2007.

Jain, S. K.: Investigating the behavior of statistical indices for performance assessment of a reservoir, J. Hydrol., 391, 90–96, 2010.

Kjeldsen, T. R. and Rosbjerg, D.: Choice of reliability, resilience and vulnerability estimators for risk assessments of water resources systems, Hydrolog. Sci. J., 49, 755–767, 2004.

Klemes, V., Srikanthan, R., and McMahon, T. A.: Long-memory flow models in reservoir analysis: what is their practical value?, Water Resour. Res., 17, 737–751, 1981.

Lence, B. J., Furst, J., and Matheson, S.: Distributive fairness as a criterion for sustainability evaluative measures and application to project selection, Int. J. Sust. Dev. World, 4, 245–258, 1997.

Loucks, D. P.: Quantifying trends in system sustainability, Hydrolog. Sci. J., 42, 513–530, 1997.

Loucks, D. P. and van Beek, E.: Water Resources Systems Planning and Management: an Introduction to Methods, Models and Applications, United Nations Educational, Scientific and Cultural Organization (UNESCO), Paris, 2005.

McMahon, T. A., Adeloye, A. J., and Sen-Lin, Z.: Understanding performance measures of reservoirs (Amsterdam), J. Hydrol., 324, 359–382, doi:10.1016/j.jhydrol.2005.09.030, 2006.

Mendoza, V. M., Villanuave, E. E., and Adem, J.: Vulnerability of basins and watersheds in Mexico to global climate change, Climate Res., 9, 139–145, 1997.

Moy, W. S., Cohon, J. L., and Revelle, C. S.: A programming model for analysis of reliability, resilience and vulnerability of a water supply reservoir, Water Resour. Res., 22, 489–498, 1986.

National Science Council of Taiwan: Taiwan Climate Change Projection and Information Platform Project (TCCIP), Taipei, Taiwan, 2010.

Palmer, W. C.: Meteorological drought, Research Paper 45, Weather Bureau, US Dept. of Commerce, Washington, DC, 1965.

Ray, P. A., Vogel, R. M., and Watkins, D. W.: Robust optimization using a variety of performance indices, in: World Environmental and Water Resources Congress, ASCE, Providence, RI, 4710–4719, 16–20 May 2010.

Richardson, C. W.: Stochastic simulation of daily precipitation, temperature, and solar-radiation, Water Resour. Res., 17, 182–190, 1981.

Sandoval-Solis, S., McKinney, D., and Loucks, D.: Sustainability index for water resources planning and management, J. Water Res. Pl.-ASCE, 137, 381–390, 2011.

Schilling, J., Freier, K. P., Hertig, E., and Scheffran, J.: Climate change, vulnerability and adaptation in North Africa with focus on Morocco, Agr. Ecosyst. Environ., 156, 12–26, 2012.

Schubert, S.: A weather generator based on the European “Grosswetterlagen”, Climate Res., 4, 191–202, 1994.

Selker, J. S. and Haith, D. A.: Development and testing of single-parameter precipitation distributions, Water Resour. Res., 26, 2733–2740, 1990.

Takeuchi, K., Hamlin, M., Kundzewicz, Z. W., Rosbjerg, D., and Simonovic, S. P.: Sustainable reservoir development and management, IAHS, 251, Wallingford,Oxfordshire, 1998.

Tseng, H. W., Yang, T. C., Kuo, C. M., and Yu, P. S.: Application of multi-site weather generators for investigating wet and dry spell lengths under climate change: a case study in Southern Taiwan, Water Resour. Manag., 26, 4311–4326, doi:10.1007/s11269-012-0146-6, 2012.

Tung, C. P. and Haith, D. A.: Global-warming effects on New York streamflows, J. Water Res. Pl.-ASCE, 121, 216–225, 1995.

Vano, J. A., Voisin, N., Cuo, L., Hamlet, A. F., Elsner, M. M., Palmer, R. N., Polebitski, A., and Lettenmaier, D. P.: Climate change impacts on water management in the Puget Sound region, Washington State, USA, Climatic Change, 102, 261–286, 2010.

Woolhiser, D. A. and Pegram, G. G. S.: Maximum likelihood estimation of fourier coefficients to describe seasonal variation of parameters in stochastic daily precipitation models, J. Appl. Meteorol., 18, 34–42, 1979.

Woolhiser, D. A. and Roldan, J.: Stochastic daily precipitation models, 2. A comparison of distribution of amounts, Water Resour. Res., 18, 1461–1468, 1982.

Woolhiser, D. A. and Roldan, J.: Seasonal and regional variability of parameters for stochastic daily precipitation models, Water Resour. Res., 22, 965–978, 1986.

Yu, P. S. and Yang, T. C.: Fuzzy multi-objective function for rainfall-runoff model calibration, J. Hydrol., 238, 1–14, 2000.

Yu, P. S., Yang, T. C., and Wu, C. K.: Impact of climate change on water resources in Southern Taiwan, J. Hydrol., 260, 161–175, 2002.

Yu, P. S., Kuo, C. C., Leu, J. M., and Sung, C. W.: The influence of climate change on meteorological drought characteristic in Taiwan, in: Conference on Water Observation and Information System for Decision Support, Ohrid, FY Republic of Macedonia, Climate, 1–8, 25–29 May, 2004.

Yu, P. S., Yang, T. C., and Kuo, C. C.: Evaluating long-term trends in annual and seasonal precipitation in Taiwan, Water Resour. Manag., 20, 1007–1023, 2006.

Yu, P. S., Tseng, H. W., and Chen, S. T.: Impact of climate change on agriculture water resources for paddy rice over Southern Taiwan, in: International Congress on Environmental Modelling and Software, Ottawa, Ontario, Canada, 5–8 July 2010.

Zongxue, X., Jinno, K., Kawanura, A., Takesaki, S., and Ito, K.: Performance risk analysis for Fukuoka water supply system, Water Resour. Manag., 12, 13–30, 1998.

Table 1. Summary of selected GCMs in this study.

Country	Center	Model	Abbreviation	Resolution
Australia	CSIRO	Mk3.5	CSIRO-Mk3.5	T63, L18
Canada	CCCma	CGCM3.1(T63)	CGCM3.1(T63)	T63, L31
Germany	MPI-M	ECHAM5-OM	ECHAM5/MPI-OM	T63, L31
USA	GFDL	CM2.0	GFDL-CM2.0	2.5° × 2°, L24
Japan	MRI	CGCM2.3.2	MRI-CGCM2.3.2	T42, L30
Japan	NIES	MIROC3.2	MIROC3.2(hires)	T106, L56
USA	GFDL	CM2.1	GFDL-CM2.1	2.5° × 2°, L24

Table 2. Change rates (%) of monthly rainfall from the baseline period to the future period for different GCMs.

GCM	Jan	Feb	Mar	Apr	May	Jun	Jul	Aug	Sep	Oct	Nov	Dec
CGCM3.1(T63)	−13.53	40.67	−4.26	−12.92	8.27	−18.13	−18.98	−2.34	18.14	−17.81	−31.99	−22.35
CSIRO-Mk3.5	−30.99	−21.97	−16.76	−10.28	−9.48	21.34	4.87	2.76	19.91	57.34	25.99	−23.24
GFDL-CM2.0	−6.87	2.80	−4.57	−7.80	−20.09	19.03	−17.17	−6.49	20.69	1.93	2.18	−0.49
GFDL-CM2.1	50.39	−36.44	−21.03	−6.00	−10.77	16.99	34.58	12.23	−32.54	−55.42	56.81	−5.56
MRI-CGCM2.3.2	−18.01	−52.24	−38.00	−1.54	15.64	3.77	30.95	13.89	18.65	−8.44	−46.89	−31.65
MIROC3.2(hires)	0.80	13.20	−36.33	−33.01	−27.60	8.10	−1.13	−15.19	12.94	39.70	−23.24	10.22
ECHAM5/MPI-OM	9.67	−17.94	−12.82	25.39	3.80	5.94	−24.52	−35.88	2.52	−21.81	−15.21	19.29

Table 3. Change of monthly mean temperature (˚C) from the baseline period to the future period for different GCMs.

GCM	Jan	Feb	Mar	Apr	May	Jun	Jul	Aug	Sep	Oct	Nov	Dec
CGCM3.1(T63)	0.70	0.64	0.98	1.61	1.29	1.44	1.45	1.40	1.66	1.34	1.44	1.07
CSIRO-Mk3.5	0.22	0.75	1.25	0.97	1.66	1.38	1.15	1.17	1.30	1.23	1.20	0.48
GFDL-CM2.0	0.99	1.13	0.81	0.50	0.72	0.66	1.38	1.03	0.99	0.47	0.77	1.30
GFDL-CM2.1	1.52	0.50	0.79	0.90	1.02	1.08	1.21	0.93	1.09	1.18	1.56	0.80
MRI-CGCM2.3.2	0.38	1.08	0.85	0.85	1.16	1.21	0.97	0.83	0.93	0.79	0.70	0.47
MIROC3.2(hires)	1.45	1.24	1.03	1.53	1.70	1.55	1.62	1.63	1.55	1.42	1.41	1.56
ECHAM5/MPI-OM	1.25	0.46	0.68	0.90	0.94	0.62	1.23	1.04	1.03	0.56	1.20	1.34

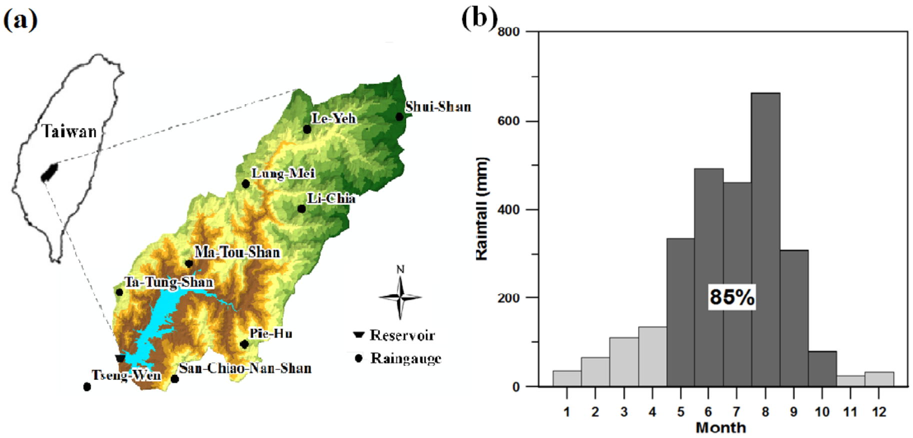

Fig. 1. (a) The catchment of Tsengwen Reservoir and **(b)** mean monthly rainfalls.

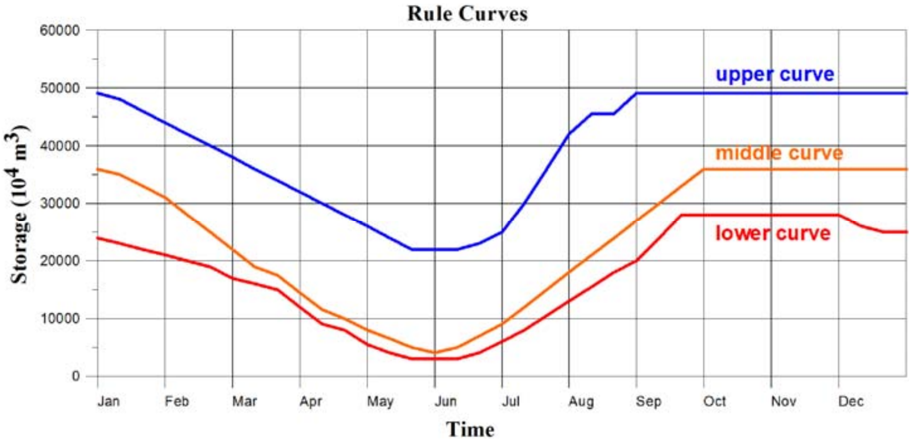

Fig. 2. The rule curves of Tsengwen Reservoir.

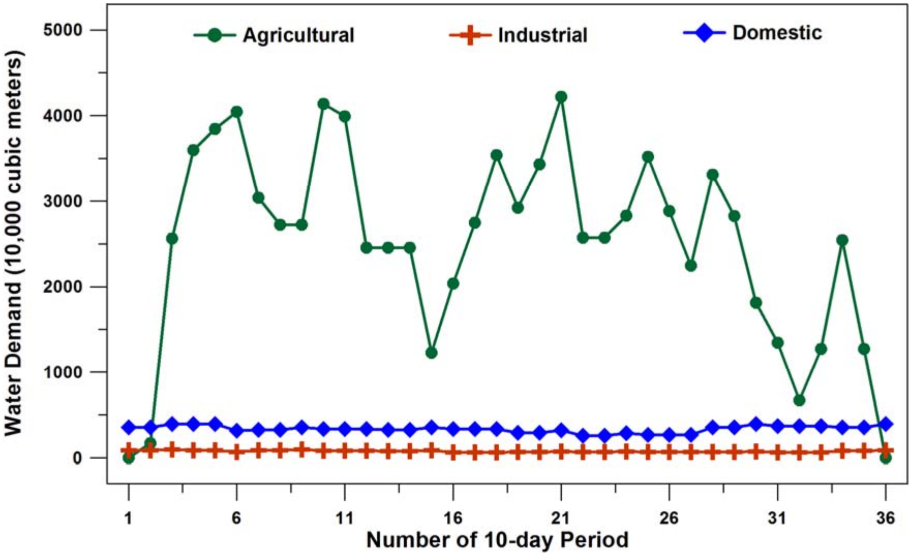

Fig. 3. Demands of agricultural, industrial, and domestic water uses.

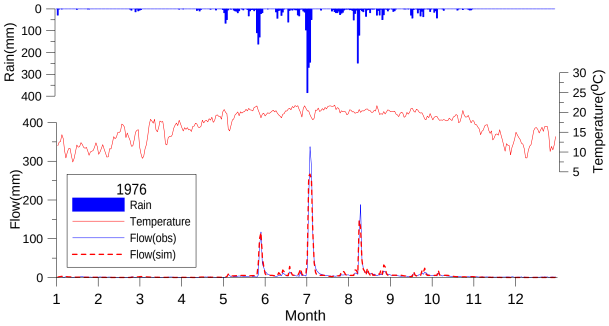

(a) Calibration results in 1976

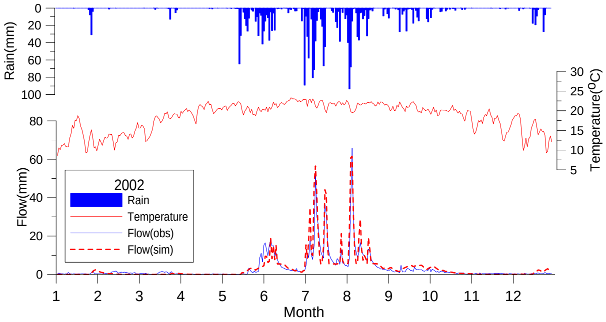

(b) Verification results in 2002

Fig. 4. Calibration and verification results for the HBV-based hydrological model in 1976 and 2002, respectively (DOY: Day of Year).

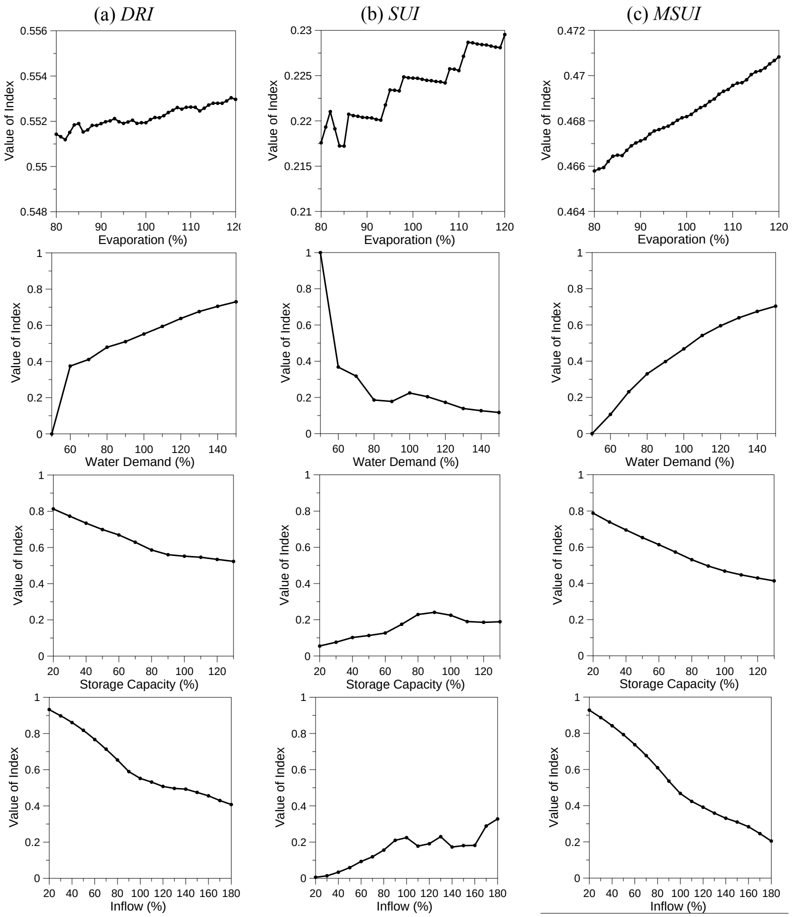

Fig. 5. Analysis results of monotonic behavior for each index.

HESSD
9, 12395–12433, 2012

Drought risk assessment of water resources systems

T. C. Yang et al.

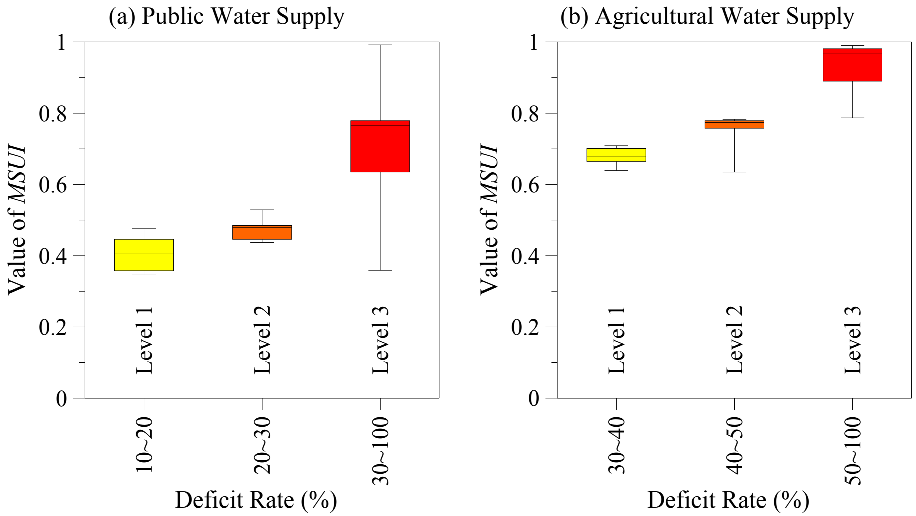

Fig. 6. Box plots of MSUI value for each drought level.

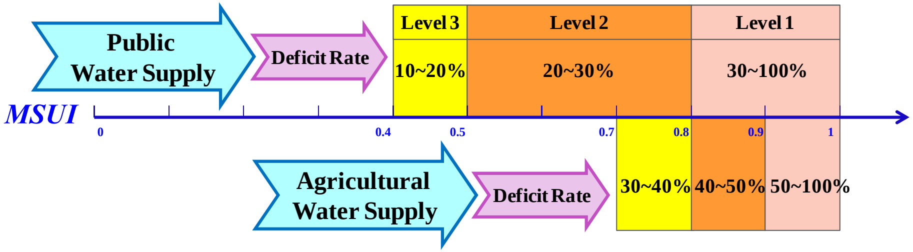

Fig. 7. Drought levels and their corresponding MSUI values and deficit rates.

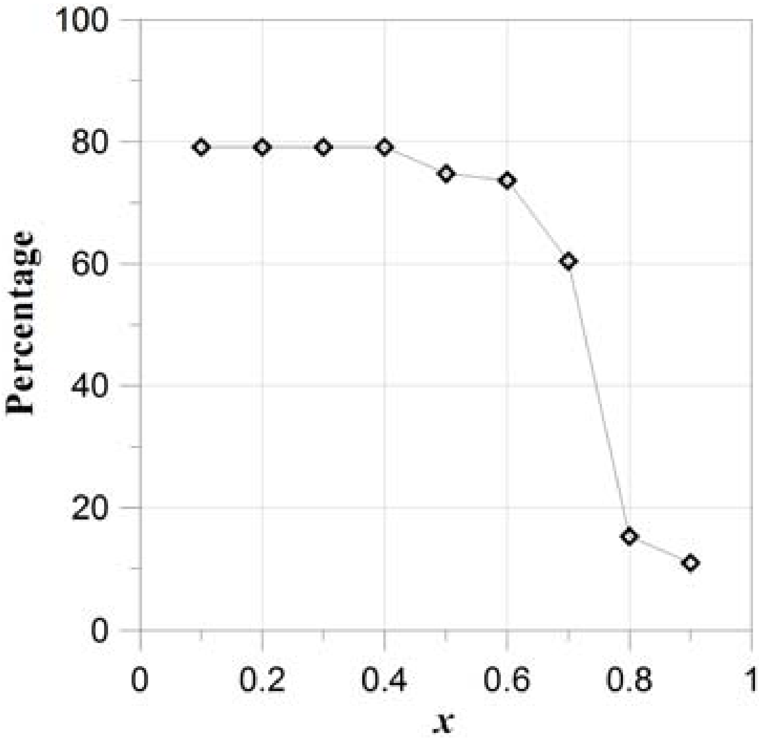

Fig. 8. Percentage of the 10-day number with MSUI ≥ x to the 10-day number of historical drought.

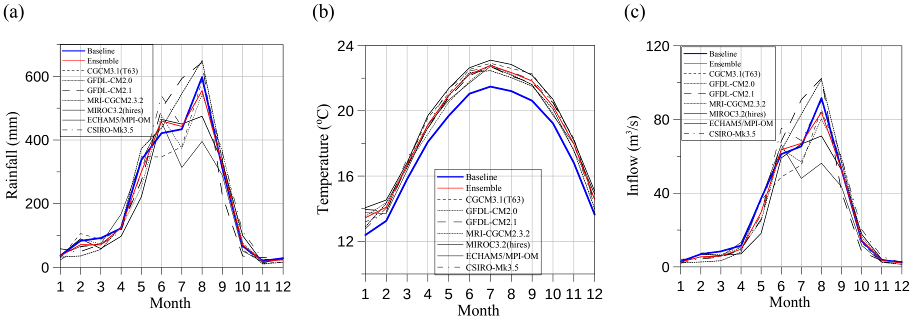

Fig. 9. Projected **(a)** mean monthly rainfalls, **(b)** average monthly mean temperatures and **(c)** average monthly mean inflows by using different GCMs.

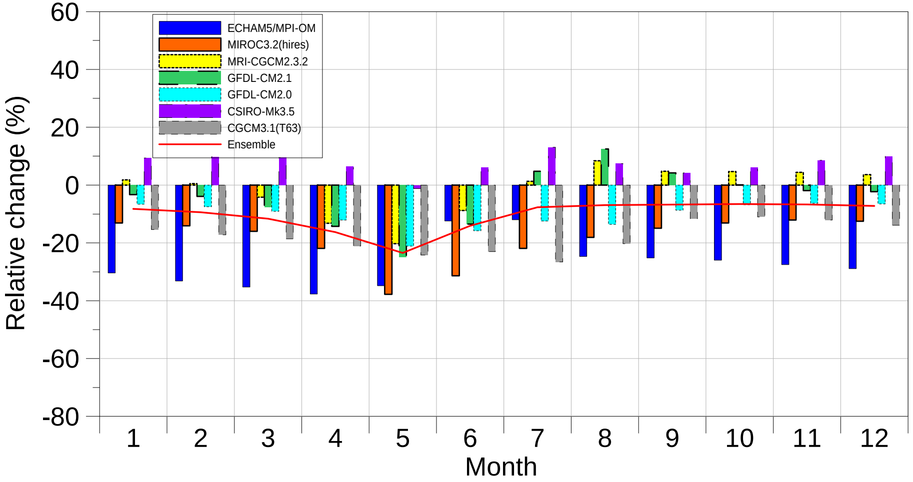

Fig. 10. Percentage changes of mean monthly storage from the baseline period to the future period.

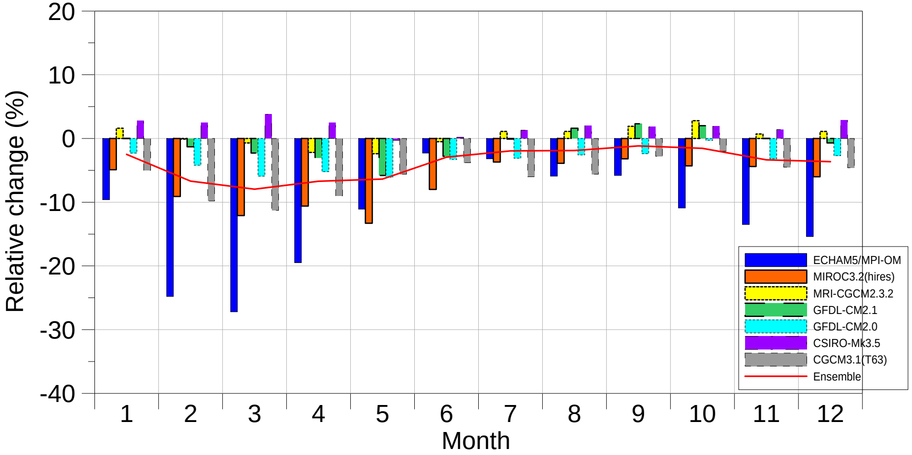

Fig. 11. Percentage changes of mean monthly water supply amount from the baseline period to the future period.

HESSD
9, 12395–12433, 2012

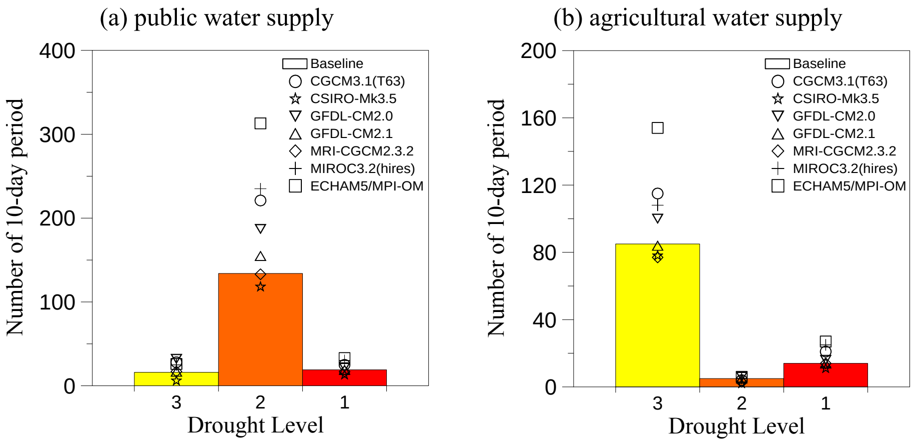

Fig. 12. Numbers of 10-day period for different drought levels by using different GCMs for **(a)** public water supply and **(b)** agricultural water supply.